ONLINE FIRST

REPORTS OF PRACTICAL ONCOLOGY AND RADIOTHERAPY

ISSN: 1507-1367

e-ISSN: 2083-4640

Dose difference between anisotropic analytical algorithm (AAA) and Acuros XB (AXB) caused by target's air content for volumetric modulated arc therapy of head and neck cancer

Authors: Takaaki Ito, Hajime Monzen, Kazuki Kubo, Hiroyuki Kosaka, Yuya Yanagi, Yusuke Sakai, Masahiro Inada, Hiroshi Doi, Yasumasa Nishimura

DOI: 10.5603/RPOR.a2023.0032

Article type: Research paper

Published online: 2023-06-13

Dose difference between anisotropic analytical algorithm (AAA) and Acuros XB (AXB) caused by target's air content for volumetric modulated arc therapy of head and neck cancer

10.5603/RPOR.a2023.0032

Takaaki Ito[1, 2], Hajime Monzen[1], Kazuki Kubo[1], Hiroyuki Kosaka[1], Yuya Yanagi[1], Yusuke Sakai[1], Masahiro Inada[3], Hiroshi Doi[3], Yasumasa Nishimura[3]

[1]*Department of Medical Physics, Graduate School of Medical Sciences, Kindai University, Osakasayama, Osaka, Japan*

[2]*Department of Radiological Technology, Kobe City Nishi-Kobe Medical Center, Kobe, Hyogo, Japan*

[3]*Department of Radiation Oncology, Faculty of Medicine, Kindai University, Osakasayama, Osaka, Japan*

Corresponding author: Hajime Monzen, Ph.D., Department of Medical Physics, Graduate School of Medical Sciences, Kindai University, 377-2 Onohigashi, Osakasayama, Osaka, 5898511, Japan, tel: +81-72-366-0221; e-mail: hmon@med.kindai.ac.jp

Abstract

Background: We clarified the dose difference between the anisotropic analytical algorithm (AAA) and Acuros XB (AXB) with increasing target's air content using a virtual phantom and clinical cases.

Material and methods: Whole neck volumetric modulated arc therapy (VMAT) plan was transferred into a virtual phantom with a cylindrical air structure at the center. The diameter of the air structure was changed from 0 to 6 cm, and the target's air content defined as the air/planning target volume (PTV) in percent (air/PTV) was varied. VMAT plans were recalculated by AAA and AXB with the same monitor unit (MU) and multi-leaf collimator (MLC) motions. The dose at each air/PTV (5%–30%) was compared between each algorithm with $D_{98\%}$, $D_{95\%}$, $D_{50\%}$ and $D_{2\%}$ for the PTV. In addition, MUs were also compared with the same MLC motions between the $D_{95\%}$ prescription with AAA ($AAA\_D_{95\%}$), $AXB\_D_{95\%}$, and the prescription to 100% minus air/PTV ($AXB\_D_{100\%-air/PTV}$) in clinical cases of HNC.

Results: When air/PTV increased (5–30%), the dose differences between AAA and AXB for $D_{98\%}$, $D_{95\%}$, $D_{50\%}$ and $D_{2\%}$ were 3.08–15.72%, 2.35–13.92%, 0.63–4.59%, and 0.14–6.44%, respectively. At clinical cases with air/PTV of 5.61% and 28.19%, compared to $AAA\_D_{95\%}$, the MUs differences were, respectively, 2.03% and 6.74% for $AXB\_D_{95\%}$ and 1.80% and 0.50% for $AXB\_D_{100\%-air/PTV}$.

Conclusion: The dose difference between AAA and AXB increased as the target's air content increased, and $AXB\_D_{95\%}$ resulted in a dose escalation over $AAA\_D_{95\%}$ when the target's air content was ≥ 5%. The $D_{100\%-air/PTV}$ of PTV using AXB was comparable to the $D_{95\%}$ of PTV using AAA.

Key words: anisotropic analytical algorithm (AAA); Acuros XB (AXB); head and neck cancer (HNC)

Introduction

In external radiotherapy for regions such as the head and neck, where air and bone

heterogeneity are high, the uncertainty of the calculated dose distribution depends on the accuracy of the calculation algorithm as one factor [1–5]. To reduce this uncertainty, it is crucial that an accurate calculation algorithm is selected.

The Eclipse treatment planning system (Varian Medical Systems, Palo Alto, CA, United States) provides two algorithms to calculate dose: the anisotropic analytical algorithm (AAA) and Acuros XB (AXB). AAA applies simplified density scaling of the dose kernel to heterogeneous media using convolution and superposition [6]. AXB uses the linear Boltzmann transport equation (LBTE) to calculate the behavior of radiation particles as they travel through and interact with matter [7, 8]. In air, AAA overestimates doses, whereas AXB doses are in good agreement with those of Monte Carlo simulations and actual measurements [9–12]. Additionally, in high-density metal structures, Pawalowski et al. reported that AAA overestimates doses by more than 10%, AXB doses are in good agreement with Monte Carlo simulations and actual measurements [12]. Therefore, AXB is recommended for accurate dose calculation of regions with heterogeneity, such as air and bone in the head and neck region [13–15]. However, Israngkul et al. reported that the dose delivered to 95% volume of targets ($D_{95\%}$) calculated by the AXB were reduced by approximately 28% compared with the AAA in the case of a small target and large air content for volumetric modulated arc therapy (VMAT) of pituitary carcinoma [14]. Therefore, using the same dose prescription method (i.e. normalizing at $D_{95\%}$) may result in a dose escalation when the dose calculation algorithm for VMAT plan is changed from AAA to AXB for head and neck cancer (HNC). When changing the dose calculation algorithm used in clinical to AXB, it is important to ensure that the doses delivered to targets using AXB do not greatly deviate from using AAA. Because the doses to target reported in previous papers

were calculated based on AAA or similar algorithms. For example, RTOG-0522, one of the evidence-based medicines for HNC, adopted the dose prescription for $D_{95\%}$ of targets using AAA or similar algorithms [16]. In this study, we clarified the dose difference between AAA and AXB caused by the target's air content in the VMAT planning of HNC. We also investigated that the dose parameters of targets using AXB were equivalent to the $D_{95\%}$ of targets using AAA, even as the target's air content increased.

Materials and methods

Virtual phantom with air structure for VMAT planning of the whole neck

For the head and neck region, a water-equivalent cylindrical virtual phantom was created in the treatment planning system, Eclipse ver. 15.6, with a diameter of 26 cm, length of 50 cm, and slice thickness of 2 mm. We transferred the plan and the structure, including the planning target volume (PTV) contoured by the radiation oncologist, of a patient who underwent whole neck VMAT at our institution to the center of this cylindrical phantom. Whole neck VMAT in conjunction with the simultaneous integrated boost (SIB) method for the prescribed PTV dose of 70 Gy (PTV_{70Gy}) was delivered via 2.12 Gy per fraction. 95% volume of PTV_{70Gy} was covered by the 100% of the prescribed dose. The cylindrical air structure (–1000 Hounsfield unit: HU) of 50 cm in length was placed at the center of the cylinder phantom [14, 17], and the diameter of the air structure was incremented by 1 cm from 0 to 6 cm (Fig. 1). The target's air content was varied by changing the air in PTV_{70Gy} divided by PTV_{70Gy} in percent (air/PTV) as follows: 0%, 1.6%, 6.4%, 13.9%, 23.4%, 34.3%, and 46.2%. The isocenter was set at the center of PTV_{70Gy}. The gantry rotation angle was set from 181° to 179° with collimator angles of 20° and 340°. The multi-leaf collimator (MLC) (Millennium

120) in TrueBeam (Varian Medical Systems, Palo Alto CA, United States) was employed. The X-ray energy was 6 MV, and the maximum dose rate was 600 monitor unit (MU)/min. Dose-to-medium was used for AXB dose calculations, and the grid size for dose calculations was 2 mm [18]. The accuracy of AAA and AXB dose calculations at our institution had been adjusted to agree with measured values within 1~2% in representative field sizes at the commissioning.

Dose difference with increasing target's air content

For each target's air content, the dose differences between AAA and AXB were obtained in the cylindrical virtual phantom (Section 2.1). The whole neck VMAT plans transferred to the cylindrical virtual phantom were recalculated by AAA and AXB with the same MU and MLC motions [13] while changing the air/PTV (0%, 1.6%, 6.4%, 13.9%, 23.4%, 34.3%, and 46.2%). $D_{98\%}$, $D_{95\%}$, $D_{50\%}$, and $D_{2\%}$ of PTV_{70Gy} were compared between AXB and AAA. D_x is the dose covering x% of the volume.

2.3 Differences of dose indices between AAA and AXB

For each target's air content, the dose differences between $D_{95\%}$ of PTV_{70Gy} using AAA and $D_{95\%}$, $D_{50\%}$ and $D_{100\%\text{-air/PTV}}$ of PTV_{70Gy} using AXB were obtained in the cylindrical virtual phantom (see *Virtual phantom with air structure for VMAT planning of the whole neck*). The whole neck VMAT plans transferred to the cylindrical virtual phantom were calculated by the $D_{95\%}$ prescription using AXB for the PTV_{70Gy}, and recalculated by AAA with the same MLC motions [13] while changing the air/PTV (0%, 1.6%, 6.4%, 13.9%, 23.4%, 34.3%, and 46.2%). For each target's air content, the MU calculated by the $D_{95\%}$ prescription using AXB were 829.6, 830.3, 838.2, 880.0, 931.4, 969.2 and

1001.1 MU. $D_{100\%\text{-air/PTV}}$ indicates doses of 100% of PTV volume minus the air/PTV. $D_{100\%\text{-air/PTV}}$ was developed from the results of Section 2.2, where AAA produced greater values than AXB with $D_{98\%}$, $D_{95\%}$, $D_{50\%}$, and $D_{2\%}$ for PTV_{70Gy}, and the difference increased as the target's air content increased.

2.4 ***Dose escalation or underdose with air for each prescription method: clinical cases***

Three clinical VMAT plans with the target's air contents of 5.61% (whole neck), 17.02% (larynx), and 28.19% (nasopharynx) were used to evaluate MU for each dose prescription calculated by AAA and AXB. There were differences at the dose to water and the dose to medium between AAA and AXB, and the dose distributions could not be simply compared on the treatment planning systems [17]. Therefore, MUs were calculated for each prescription method using AAA and AXB under the same optimizations and MLC motions at each clinical case because MU differences were used to evaluate dose escalation or underdose for each dose prescription using AXB compared to the conventional $AAA\_D_{95\%}$. The same MU leads to the same doses and, thus, a high MU indicates a dose escalation and a low MU indicates an underdose compared to the conventional $AAA\_D_{95\%}$ [13]. MUs were obtained with the $D_{95\%}$ dose prescription method for PTV_{70Gy} using AAA ($AAA\_D_{95\%}$) and with the following dose prescription methods for PTV_{70Gy} using AXB: (1) $D_{95\%}$ dose prescription ($AXB\_D_{95\%}$), (2) $D_{50\%}$ dose prescription ($AXB\_D_{50\%}$), and (3) the 100% dose prescription method to 100% of PTV volume minus the air/PTV ($AXB\_D_{100\%\text{-air/PTV}}$). $AXB\_D_{100\%\text{-air/PTV}}$ was developed from the relationship between the target's air content and dose calculated by the algorithms (see *Differences of dose indices between AAA and AXB*). The PTV volume in clinical cases were 419.1 cm^3 (whole neck), 102.8 cm^3 (larynx), and 192.6

cm^3 (nasopharynx). The air region was automatically delineated from –1024 to –150 HU [19]. This study was conducted in accordance with the Declaration of Helsinki (as revised in 2013). We had received informed consent from all participants in the study. The study was approved by the ethics committee of the Kobe City Nishi-Kobe Medical Center (institutional review board number: 2022–23).

Results

3.1 Dose differences with increasing target's air content

The dose differences between the two calculation algorithms as a function of the target's air content are shown in Figure 2. AAA produced greater values than AXB with $D_{98\%}$, $D_{95\%}$, $D_{50\%}$, and $D_{2\%}$ for PTV_{70Gy}, and the difference increased as the target's air content increased. The dose differences between AXB and AAA with $D_{98\%}$, $D_{95\%}$, $D_{50\%}$, and $D_{2\%}$ for PTV_{70Gy} were 3.08%–15.72%, 2.35%–13.92%, 0.63%–4.59%, and 0.14%–6.44% as the target's air content increased from 5% to 30%. The dose differences were larger at near minimum doses ($D_{98\%}$) and $D_{95\%}$ than at $D_{50\%}$ and near maximum dose ($D_{2\%}$) with small increases in the target's air content. Furthermore, the dose differences at $D_{98\%}$ and $D_{95\%}$ increased linearly, while those at $D_{50\%}$ and $D_{2\%}$ increased logarithmically with increasing target's air content.

3.2 *Differences of dose indices between AAA and AXB*

The dose differences between $D_{95\%}$ of PTV_{70Gy} using AAA and $D_{95\%}$, $D_{50\%}$ and $D_{100\%\text{-air/PTV}}$ of PTV_{70Gy} using AXB as a function of the target's air content were shown in Figure 3. $D_{95\%}$, $D_{50\%}$ and $D_{100\%\text{-air/PTV}}$ were the dose parameters in section *Dose escalation or underdose with air for each prescription method: clinical cases* to use as the dose

prescription volume. Compared to the $D_{95\%}$ of PTV_{70Gy} using AAA at the target's air content of 5%, the corresponding $D_{95\%}$ of PTV_{70Gy} using AXB was –1.04%, the corresponding $D_{50\%}$ of PTV_{70Gy} using AXB was 6.11%, and the corresponding $D_{100\%-air/PTV}$ of PTV_{70Gy} using AXB was –1.12%. Compared to the $D_{95\%}$ of PTV_{70Gy} using AAA at the target's air content of 30%, the corresponding $D_{95\%}$ of PTV_{70Gy} using AXB was –16.09%, the corresponding $D_{50\%}$ of PTV_{70Gy} using AXB was 3.58%, and the corresponding $D_{100\%-air/PTV}$ of PTV_{70Gy} using AXB was –0.97%.

The dose differences between $D_{95\%}$ of PTV_{70Gy} using AAA and $D_{100\%-air/PTV}$ of PTV_{70Gy} using AXB were within ±1%, when the target's air content was ≥ 5%. In contrast, the $D_{95\%}$ of PTV_{70Gy} using AXB was lower than that of $D_{95\%}$ of PTV_{70Gy} using AAA caused by increasing target's air content > 5%. Additionally, the $D_{50\%}$ of PTV_{70Gy} using AXB was higher than $D_{95\%}$ of PTV_{70Gy} using AAA, especially as the target's air content decreased.

3.3 Dose escalation or underdose with air for each prescription method: clinical cases

The MUs of AAA_$D_{95\%}$, AXB_$D_{95\%}$, AXB_$D_{50\%}$, and AXB_$D_{100\%-air/PTV}$ for three clinical cases with different target's air contents are shown in Table 1. In all cases, the MU of AXB_$D_{95\%}$ was higher than that of AAA_$D_{95\%}$, and the difference increased as the target's air content increased (maximum of 6.74% for the nasopharynx). In contrast, the MU of AXB_$D_{50\%}$ was lower than that of AAA_$D_{95\%}$, and the difference increased as the target's air content decreased (minimum of -1.69% for the whole neck). The MU of AXB_$D_{100\%-air/PTV}$ was in agreement with that of AAA_$D_{95\%}$ (±2%) in all cases, and it was unaffected by the target's air content ≥ 5%.

Discussion

In this study, we clarified the dose difference between AAA and AXB with increasing target's air content using a virtual phantom and clinical cases (Fig. 2, Fig. 3, and Tab. 1). We found that the $D_{100\%\text{-air/PTV}}$ of PTV using AXB was comparable to the $D_{95\%}$ of PTV using AAA when the target's air content was ≥ 5%.

The dose difference increased as the target's air content increased (Fig. 2) owing to the lack of scattering with AAA and occurrence of scattering with AXB [8, 20]. The correlation shown in Figure 2 can be used to estimate the dose difference between calculation algorithms. In particular, the differences at near minimum dose ($D_{98\%}$) and $D_{95\%}$ were larger than those at $D_{50\%}$ and near maximum dose ($D_{2\%}$), similar to the results reported by Israngkul et al. [14]. It means that the dose difference between the $D_{95\%}$ prescription and others becomes more pronounced. Although the dose differences between AAA and AXB for IMRT and VMAT decrease because of dose compensation from out of field [9, 17], the dose differences between calculation algorithms are large when the target's air content is large.

We determined the relationship between the dose differences of $D_{95\%}$, $D_{50\%}$ and $D_{100\%\text{-air/PTV}}$ of PTV_{70Gy} using AXB compared to $D_{95\%}$ of PTV_{70Gy} using AAA and the target's air content, as shown in Figure 3. The dose differences of PTV_{70Gy} between $D_{95\%}$ using AAA and $D_{100\%\text{-air/PTV}}$ using AXB were within ±1%, even as the target's air content was ≥ 5%. The relationship shown in Figure 3 can be used to estimate the occurrence of a dose escalation or underdose. The MUs of AAA_$D_{95\%}$, AXB_$D_{95\%}$, AXB_$D_{50\%}$, and AXB_$D_{100\%\text{–air/PTV}}$ for three clinical cases with different target's air contents were shown in Table 1. The MU differences between AXB_$D_{100\%\text{–air/PTV}}$ and AAA_$D_{95\%}$ were within

±2%, even as the target's air content increased. These results, similar to those of Section 3.2, indicate that AXB_$D_{100\%–air/PTV}$ can be adapted not only for virtual phantoms but also for clinical cases with target's air content ≥ 5%.

The difference in dosage between AAA and AXB caused by an air cavity present within the PTV depends on various factors such as the size and distance of the cavity, field size, and the density of the surrounding medium [8, 13, 14, 21]. Rana et al. reported that smaller field sizes and longer cavity distances result in larger AAA and AXB dose differences in the air regions for beam from a gantry angle of 0 degree [21]. The dose index $D_{100\text{-}air/PTV}$ of PTV using AXB evaluates the dose of the region excluding air cavities from the PTV. As a result, it showed agreement within 1% of the $D_{95\%}$ of PTV using AAA, even in cases of smaller field sizes for laryngeal cancer. Therefore, only the target's air content needs to be checked and small target sizes, such as the larynx and nasopharynx,, tend to have a larger target's air content. It should be noted that it is not dose escalation compared to the conventional AAA_$D_{95\%}$. Other methods have been reported to improve the accuracy of dose calculation in HNC [22–24]. Asher et al. proposed removing the air from the PTV as the air cavity within the larynx presents a challenge for inverse planning software. The software tries to "push" dose into the air to achieve adequate target coverage, especially when using more complex dose calculation algorithms [22]. However, removing the air cavity may lead to underdosing of the treatment volumes at the interface between air and tissue [25], which may increase the risk of cancer recurrence in the normal tissue adjacent to the air-tissue interface [26]. Moreover, the procedure of omitting the air cavities from the targets would be burdensome to the planner.

When changing from the conventional method of AAA to AXB for targets with large air

contents, such as the head and neck, evaluations similar to our study must be performed and discussed with the radiation oncologist, radiation technologists, and medical physicists to prevent a dose escalation or underdose. Although the AXB algorithm is known to be more accurate, this study compared the doses and MU calculated by AXB to those calculated by the AAA algorithm used as a reference. Our study focuses on the transitional period when the dose calculation algorithm was changed from AAA to AXB. In clinical practice, AXB would be the ideal algorithm to use as a reference.

Conclusions

In HNC VMAT, the dose difference between AAA and AXB increased as the target's air content increased, and changing from conventional AAA_$D_{95\%}$ to AXB_$D_{95\%}$ had the risk of dose escalation. The $D_{100\%\text{-air/PTV}}$ of PTV using AXB was comparable to the $D_{95\%}$ of PTV using AAA when the target's air content is ≥ 5%.

Acknowledgments

We thank Edanz (https://jp.edanz.com/ac) for editing a draft of this manuscript.

Conflicts of interest

None declared.

Funding

This work was supported partly by Japan Society for the Promotion of Science (JSPS) KAKENHI (grant number: 20K08093).

Author contribution

T.I., H.M. were associated with concept and design; T.I., Y.Y. and Y.S. took the

measurements. T.I., Y.Y., Y.S. and K.K. analyzed the data. T.I., H.M., M.I., H.D. and Y.N. prepared the manuscript. All authors read and approved the final manuscript.

References

1. 1. Knöös T, Ahnesjö A, Nilsson P, et al. Limitations of a pencil beam approach to photon dose calculations in lung tissue. Phys Med Biol. 1995; 40(9): 1411–1420, doi: 10.1088/0031-9155/40/9/002, indexed in Pubmed: 8532755.

2. Arnfield MR, Siantar CH, Siebers J, et al. The impact of electron transport on the accuracy of computed dose. Med Phys. 2000; 27(6): 1266–1274, doi: 10.1118/1.599004, indexed in Pubmed: 10902555.

3. Chetty IJ, Curran B, Cygler JE, et al. Report of the AAPM Task Group No. 105: Issues associated with clinical implementation of Monte Carlo-based photon and electron external beam treatment planning. Med Phys. 2007; 34(12): 4818–4853, doi: 10.1118/1.2795842, indexed in Pubmed: 18196810.

4. Reynaert N, Marck SCv, Schaart DR, et al. Monte Carlo treatment planning for photon and electron beams. Radiat Phys Chem. 2007; 76(4): 643–686, doi: 10.1016/j.radphyschem.2006.05.015.

5. Han T, Mourtada F, Kisling K, et al. Experimental validation of deterministic Acuros XB algorithm for IMRT and VMAT dose calculations with the Radiological Physics Center's head and neck phantom. Med Phys. 2012; 39(4): 2193–2202, doi: 10.1118/1.3692180, indexed in Pubmed: 22482641.

6. Fogliata A, Nicolini G, Clivio A, et al. Dosimetric validation of the anisotropic analytical algorithm for photon dose calculation: fundamental characterization in water. Phys Med Biol. 2006; 51(6): 1421–1438, doi: 10.1088/0031-9155/51/6/004, indexed in Pubmed: 16510953.

7. Han T, Mikell JK, Salehpour M, et al. Dosimetric comparison of Acuros XB deterministic radiation transport method with Monte Carlo and model-based convolution methods

in heterogeneous media. Med Phys. 2011; 38(5): 2651–2664, doi: 10.1118/1.3582690, indexed in Pubmed: 21776802.

8. Fogliata A, Nicolini G, Clivio A, et al. Dosimetric evaluation of Acuros XB Advanced Dose Calculation algorithm in heterogeneous media. Radiat Oncol. 2011; 6: 82, doi: 10.1186/1748-717X-6-82, indexed in Pubmed: 21771317.

9. Shen Z, Tan X, Li S, et al. Correlation between the γ passing rates of IMRT plans and the volumes of air cavities and bony structures in head and neck cancer. Radiat Oncol. 2021; 16(1): 134, doi: 10.1186/s13014-021-01861-y, indexed in Pubmed: 34289863.

10. Alhakeem EA, AlShaikh S, Rosenfeld AB, et al. Comparative evaluation of modern dosimetry techniques near low- and high-density heterogeneities. J Appl Clin Med Phys. 2015; 16(5): 142–158, doi: 10.1120/jacmp.v16i5.5589, indexed in Pubmed: 26699322.

11. Bush K, Gagne IM, Zavgorodni S, et al. Dosimetric validation of Acuros XB with Monte Carlo methods for photon dose calculations. Med Phys. 2011; 38(4): 2208–2221, doi: 10.1118/1.3567146, indexed in Pubmed: 21626955.

12. Pawałowski B, Ryczkowski A, Panek R, et al. Accuracy of the doses computed by the Eclipse treatment planning system near and inside metal elements. Sci Rep. 2022; 12(1): 5974, doi: 10.1038/s41598-022-10072-8, indexed in Pubmed: 35396569.

13. Kan MWK, Leung LHT, Yu PKN. Verification and dosimetric impact of Acuros XB algorithm on intensity modulated stereotactic radiotherapy for locally persistent nasopharyngeal carcinoma. Med Phys. 2012; 39(8): 4705–4714, doi: 10.1118/1.4736819, indexed in Pubmed: 22894395.

14. Israngkul-Na-Ayuthaya I, Suriyapee S, Sanghamthum T. The dosimetric comparison using anisotropic analytical algorithm (AAA) and Acuros XB algorithms in the target overlapping with air cavity of pituitary carcinoma. Ther Radiol Oncol. 2021; 5: 7–7, doi: 10.21037/tro-20-57.

15. Srivastava RP, Basta K, De Gersem W, et al. A comparative analysis of Acuros XB and the analytical anisotropic algorithm for volumetric modulation arc therapy. Rep Pract

Oncol Radiother. 2021; 26(3): 481–488, doi: 10.5603/RPOR.a2021.0050, indexed in Pubmed: 34277105.

16. Ang K, Zhang Q, Rosenthal D, et al. Randomized Phase III Trial of Concurrent Accelerated Radiation Plus Cisplatin With or Without Cetuximab for Stage III to IV Head and Neck Carcinoma: RTOG 0522. J Clin Oncol. 2014; 32(27): 2940–2950, doi: 10.1200/jco.2013.53.5633, indexed in Pubmed: 25154822.

17. Kan MWK, Leung LHT, Yu PKN. Dosimetric impact of using the Acuros XB algorithm for intensity modulated radiation therapy and RapidArc planning in nasopharyngeal carcinomas. Int J Radiat Oncol Biol Phys. 2013; 85(1): e73–e80, doi: 10.1016/j.ijrobp.2012.08.031, indexed in Pubmed: 23040220.

18. Muñoz-Montplet C, Marruecos J, Buxó M, et al. Dosimetric impact of Acuros XB dose-to-water and dose-to-medium reporting modes on VMAT planning for head and neck cancer. Phys Med. 2018; 55: 107–115, doi: 10.1016/j.ejmp.2018.10.024, indexed in Pubmed: 30471814.

19. Barateau A, Perichon N, Castelli J, et al. A density assignment method for dose monitoring in head-and-neck radiotherapy. Strahlenther Onkol. 2019; 195(2): 175–185, doi: 10.1007/s00066-018-1379-y, indexed in Pubmed: 30302507.

20. Tillikainen L, Siljamäki S, Helminen H, et al. Determination of parameters for a multiple-source model of megavoltage photon beams using optimization methods. Phys Med Biol. 2007; 52(5): 1441–1467, doi: 10.1088/0031-9155/52/5/015, indexed in Pubmed: 17301464.

21. Rana S, Rogers K, Pokharel S, et al. SU-E-T-529: Dosimetric Evaluation with Heterogeneity in Acuros XB Advanced Dose Calculation Algorithm and Anisotropic Analytical Algorithm (AAA). Med Phys. 2012; 39(6Part18): 3827–14, doi: 10.1118/1.4735618, indexed in Pubmed: 28518491.

22. Asher D, Amestoy W, Studenski MT, et al. Dosimetric comparison of intensity-modulated radiation therapy for early-stage glottic cancers with and without the air cavity in the planning target volume. Med Dosim. 2019; 44(4): 405–408, doi: 10.1016/j.meddos.2019.02.007, indexed in Pubmed: 30928177.

23. Lee AW, Ng WT, Pan JJi, et al. International guideline for the delineation of the clinical target volumes (CTV) for nasopharyngeal carcinoma. Radiother Oncol. 2018; 126(1): 25–36, doi: 10.1016/j.radonc.2017.10.032, indexed in Pubmed: 29153464.

24. Smedt B, Vanderstraeten B, Reynaert N, et al. The influence of air cavities within the PTV on Monte Carlo-based IMRT optimization. J Phys Conf Ser. 2007; 74: 021003, doi: 10.1088/1742-6596/74/1/021003.

25. Joshi CP, Darko J, Vidyasagar PB, et al. Dosimetry of interface region near closed air cavities for Co-60, 6 MV and 15 MV photon beams using Monte Carlo simulations. J Med Phys. 2010; 35(2): 73–80, doi: 10.4103/0971-6203.62197, indexed in Pubmed: 20589116.

26. Waldron JN, O'Sullivan B, Gullane P, et al. Carcinoma of the maxillary antrum: a retrospective analysis of 110 cases. Radiother Oncol. 2000; 57(2): 167–173, doi: 10.1016/s0167-8140(00)00256-5, indexed in Pubmed: 11054520.

Table 1. Comparison of the Monitor units (MUs) of AAA_$D_{95\%}$, AXB_$D_{95\%}$, AXB_$D_{50\%}$, and AXB_$D_{100\%\text{-air/PTV}}$ for clinical cases of head and neck cancer (HNC)

	Air/PTV (%)	**AAA**	**AXB**		
		$D_{95\%}$	**$D_{95\%}$**	**$D_{50\%}$**	**$D_{100\%\text{-air/PTV}}$**
Whole neck	5.61	654.78	668.09 (+2.03%)	643.70 (-1.69%)	666.59 (+1.80%)
Larynx	17.02	600.22	629.13 (+4.82%)	596.16 (-0.68%)	604.50 (+0.71%)
Nasopharynx	28.19	751.82	802.52 (+6.74%)	746.12 (-0.76%)	755.57 (+0.50%)
[MU]					

In the same MLC motions, the MUs of each dose prescription ($D_{95\%}$, $D_{50\%}$, $D_{100\%\text{-air/PTV}}$) using AXB were compared to the $D_{95\%}$ prescription using AAA in three head and neck (HNC) volumetric modulated arc therapy (VMAT) clinical cases with different air/PTV.

Figure 1. Virtual phantom with air structure for volumetric modulated arc therapy (VMAT) planning of the whole neck (blue: PTV_{70Gy}, yellow: PTV_{total}, pink: air). The diameter of the cylindrical air structure was incremented by 1 cm from 0 cm to 6 cm, and the target's air content was 0%, 1.6%, 6.4%, 13.9%, 23.4%, 34.3%, and 46.2%. PTV — planning target volume

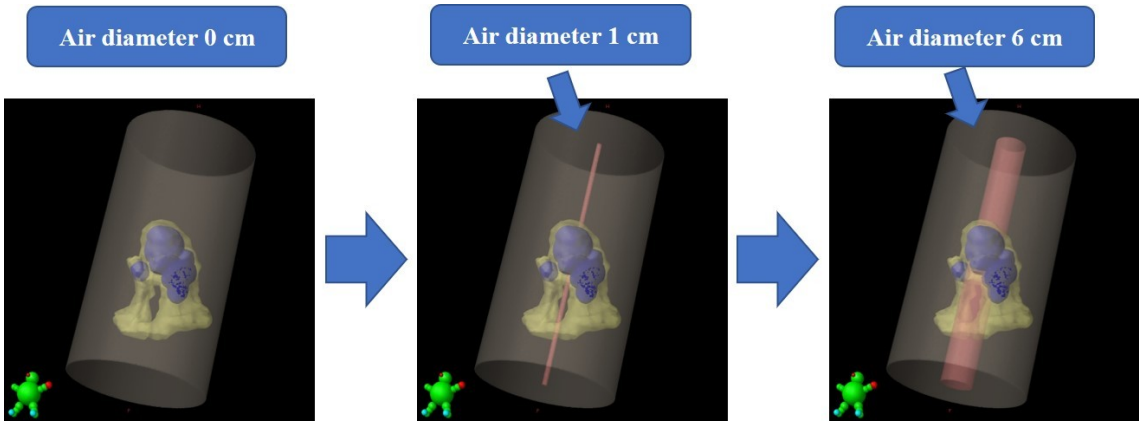

Figure 2. Dose differences between Acuros XB (AXB) and anisotropic analytical algorithm (AAA) as a function of the target's air content for prescribed planning target

volume (PTV) dose of 70 Gy (PTV_{70Gy}) with the following prescription methods: (**A**) $D_{98\%}$, (**B**) $D_{95\%}$, (**C**) $D_{50\%}$, and (**D**) $D_{2\%}$. Dotted lines in (**A**) and (**B**) are linear approximation, whereas (**C**) and (**D**) are quadratic curve approximations.

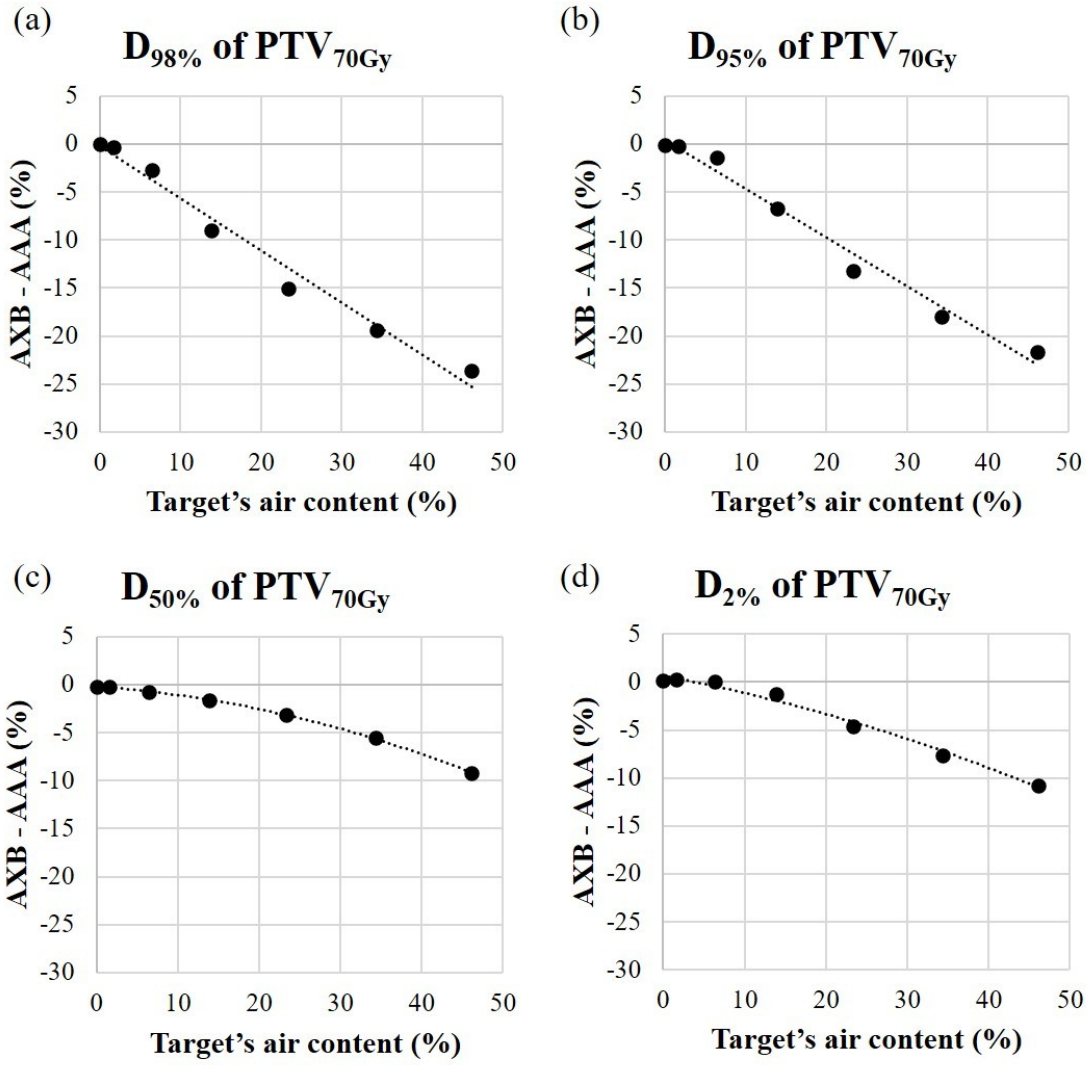

Figure 3. Dose differences between $D_{95\%}$ of prescribed planning target volume (PTV) dose of 70 Gy (PTV_{70Gy}) using anisotropic analytical algorithm (AAA) and $D_{95\%}$, $D_{50\%}$ and $D_{100\%\text{-air/PTV}}$ of PTV_{70Gy} using Acuros XB (AXB) as a function of the target's air content in the virtual phantom

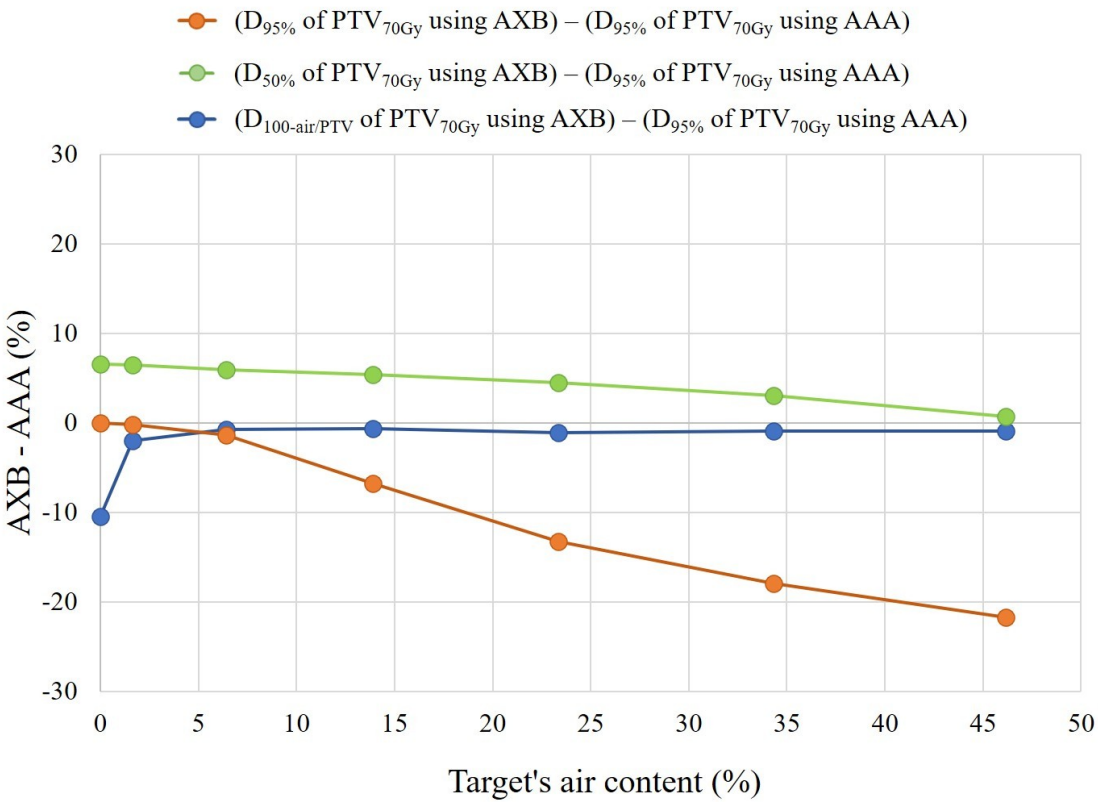
(D95% of PTV70Gy using AXB) – (D95% of PTV70Gy using AAA)
(D50% of PTV70Gy using AXB) – (D95% of PTV70Gy using AAA)
(D100-air/PTV of PTV70Gy using AXB) – (D95% of PTV70Gy using AAA)
AXB - AAA (%)
30
20
10
0
-10
-20
-30
0
5
10
15
20
25
30
35
40
45
50
Target's air content (%)